Effects of Base Fabric Parameters on the Electro-Mechanical Behavior of Piezoresistive Knitted Sensors

Shafagh Dinparast Tohidi, Andrea Zille, André Paulo Catarino, and Ana M. Rocha

***Abstract*— Strain sensors embedded into fabric structure are one of the most interesting research areas for health and engineering monitoring. In this paper, a textile-based strain sensor has been developed using an intrinsically conductive stainless steel-polyester plain knitted fabric. The influence of fabric structural parameters, such as loop length on electro-mechanical properties of sensors was studied under a tensile fatigue set. Knitted fabric structure deformation during tensile fatigue was monitored and image processed. Peak fitting of electric resistant waveforms (ERWs) and tensile fatigue versus time were performed to analyze the ERWs behavior in detail wherein the entire elongation of knit strain sensor partitioned into two distinct phases, such as loop head and loop leg sections. The results evidenced a discrepancy between loop head and loop leg elongation rate at the stretching onset and end of relaxing phase. The ERW with the higher resolution was obtained using the longest loop length along with the higher extension.**

***Index Terms*— Electrical resistance waveform, tensile fatigue, elongation rate, knitted piezoresistive sensor, strain sensors.**

I. Introduction

A PIEZORESISTIVE sensor is a device that converts variations in mechanical stress into a measurable reversible electrical output [1]. Piezoresistive sensors can also be embedded in textiles by using weaving and knitting production techniques [2]. Strain deformation, temperature, humidity and chemical reactivity are the main stimuli factors that can be converted into a measurable electrical signal [3], [4]. The growing needs of high flexibility and easy deformability in sensors have boosted the creation of a new generation of smart textile-based sensors capable of simultaneous sensing of several deformations such as tensile, shear, bending and compression [5], [6]. These intelligent and communicative structures are already used for the monitoring of athletes body performances and have a great potential to be employed in medical and electronic industries [7], [8].

Manuscript received March 11, 2018; accepted April 9, 2018. Date of publication April 12, 2018; date of current version May 9, 2018. This work was supported in part by FEDER through the COMPETE Program and in part by national funds through Portuguese Foundation for Science and Technology (FCT) under Project POCI-01-0145-FEDER- 007136 and Project UID/CTM/00264. The work of S. D. Tohidi was supported by the FCT under Grant SFRH/BD/94759/2013. The work of A. Zille was supported by FCT under Contract IF/00071/2015. The associate editor coordinating the review of this paper and approving it for publication was Prof. Tarikul Islam. *(Corresponding author: Shafagh Dinparast Tohidi.)*

The authors are with the 2C2T - Centro de Ciência e Tecnologia Têxtil, Departamento de Engenharia Têxtil, Universidade do Minho, 4800-058 Guimarães, Portugal (e-mail: shafagh.project@gmail.com; amrocha@det.uminho.pt; whiteman@det.uminho.pt; azille@2c2t.uminho.pt).

Digital Object Identifier 10.1109/JSEN.2018.2826056

Knitted fabrics are good candidates as strain-sensors because of their excellent elastic and extendable abilities in function of their loop configuration [3]. The main drawbacks of these types of strain sensors are their poor stability to the environmental conditions, low sensing accuracy and repeatability, long term fatigue, poor dimension stability and low mechanical resistance to bending and shearing [2], [9], [10]. Despite this, in the last years several research groups have developed functional prototypes with promising potential for industrial exploitation. De Rossi *et al.* [11] and Mazzoldi *et al.* [12] investigated the applications of strain-sensing textiles coating Lycra®-cotton knitted fabrics with polypyrrole and carbon loaded rubber. They observed significant variation in the electrical resistance under different stimuli such as deformation, temperature, humidity and chemical reactivity. Carpi and Rossi [13] studied the coating of conventional fabrics with a thin layer of polypyrrole. They concluded that electroactive functions can be implemented in the same woven system where vital signs and movements are converted into readable signals, which can be acquired and transmitted to elaboration devices. Zhang *et al.* [14] and Xue *et al.* [15] investigated on the theoretical model of electro-mechanical behavior (uniaxial-extension) of a conductive plain knitted fabric. The loop configurations and fabric structures were studied by a circuit network. The results demonstrated a key correlation between the contact electric resistance of the fabrics overlapping area and the sensitivity of the fabric sensors. Zhang *et al.* [16] continued their work by analyzing the extensibility and the elastic recovery. They concluded that rib structures showed better readable signal than plain ones. Silva *et al.* [17] studied textile electrodes in jersey and rib pattern as ECG measurement and respiratory activity sensors in dry and wet environments. The resulting ECG waveform allowed the extraction of the most important information in dry state, being quite excellent when the electrodes were wet. The relationship between the electrical resistance and textile force of conductive yarns was studied by Li *et al.* [18]. The experimental results revealed that the derived equations could accurately model the equivalent electrical resistance of conductive stitches of knitwear and could greatly simplify the existing models. Atalay *et al.* [19] developed a new textile-based strain sensor that was produced using an electronic flat-bed knitting machine. They embedded elastomeric yarns with different linear yarn density and silver coated polymeric yarns (as sensing element) in an interlock knitted fabric.

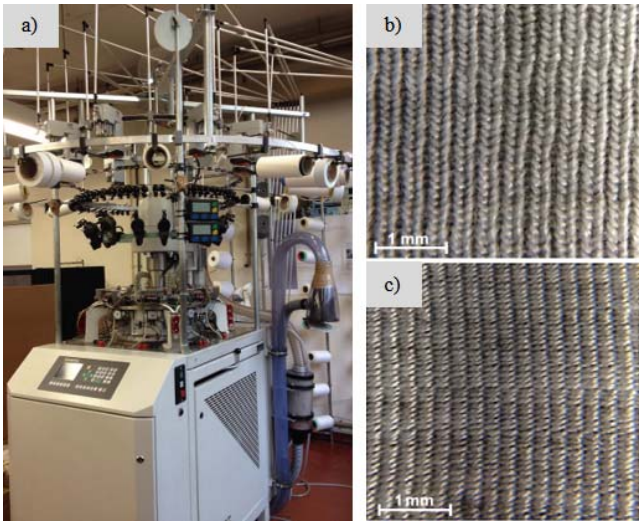

Fig. 1. a) Circular knitting machine form MERZ Company, model MBS. b) Technical Face. c) Technical back of piezoelectric knitted sensor.

The interlock structure showed the highest dimensional stability and performances compared to basic weft knitted fabric structures. Variations in elastomeric yarn input tension greatly affected the sensors' linear range and gauge factor values.

Overall, the literature data show that the optimization of knitting technology in the production of conductive fibers and yarns is the key factor for the successful application of functional knitwear sensors. However, the effects of base fabric knitting parameters on sensor characteristics are often disregarded [20].

In the present study, the effects of base fabric parameters on the electro-mechanical properties of an intrinsically conductive stainless steel-polyester composite knitted fabric were investigated under several determined extensions. The introduction of stainless steel filaments in the textile structure have proved to increase sensing ability. However, low sensitivity, repeatability and linearity are problems need to be solved. Three different loop lengths were selected for studying the influence of induced tensile fatigue on ERW under uniaxial tensile load. Moreover, an image analysis was carried out to understand the relationship between the loop elongation rates during tensile fatigue. The reliability of the sensor was tested to analyze repeatability, fabric structure deformation and loops length influence.

II. Materials And Methods

A conductive yarn 50 Nm (200 dtex), 80% polyester and 20% stainless steel fibers (BK50/1) from BEKAERT BEKINTEX ®BK with 100 Ω cm^{-1} electrical resistance was selected to produce the knit strain sensors on a circular seamless knitting machine (Model MBS, MERZ, Germany, Fig.1a). Fig.1b and 1c show the technical face and back of piezoelectric knitted sensor, respectively, in which two distinct architectures can be detected.

A uniaxial dynamometer (Houndsfield, H100KS) and a digital multimeter (Velleman, DVM840) were employed to characterize the electrical behavior of the strain sensors during the tensile fatigue test. This setting allowed the simultaneous acquisition of the electrical resistance (ER) and tensile force vs. time. Slow-speed cyclic tensile tests were performed using ten consecutive stretching (loading) (Fig.2a) and relaxing (unloading) cycles (Fig.2b) to simulate the typical application of an extension sensor. The velocity of the tensile machine crosshead was set at 60 $mm \cdot min^{-1}$ to synchronize electrical resistance magnitude with tensile force acquisition.

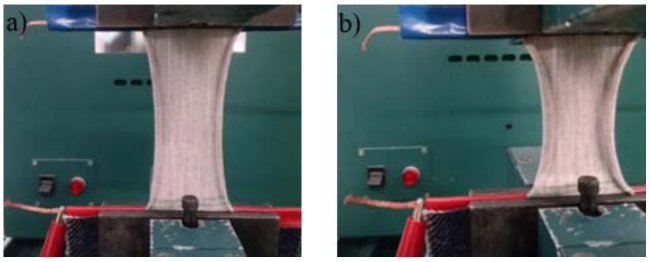

Fig. 2. Slow-speed cyclic tensile tests were performed using ten consecutive stretching a) loading and b) relaxing (unloading) cycles.

TABLE I
Sample Designation and Geometrical Characterization

Designation	Loop length (mm)	Fabric density (WPC×CPC*)
L_i† -30	2.4 (L_1)	26×15
L_i-50	2.8 (L_2)	29×14
L_i-100	3.2 (L_3)	33×13

* WPC and CPC represent the Wale and course per centimeter respectively
† i=1, 2 and 3

The knitted sensor samples (3 × 5 cm) were produced with three different loop lengths of 2.4, 2.8 and 3.2 mm (coded as L_1, L_2 and L_3, respectively) to assess their influence on the sensor responsivity. Sensors were extended in the course direction (90°) from 0% to 30%, 50% and 100% of their original length (30 mm) and kept stretched for 10 seconds interval before unloading. Table I shows the piezoelectric knitted sensor designation and geometrical characterization. To ease the comparison among ERWs with different loop length, the Time axis was presented as the ratio (%) between the time at each elongation and the total time of tensile fatigue test (Eq.1).

$$Time\,(\%) = \left(\frac{Time\ for\ each\ elongation}{Total\ test\ time}\right) \times 100 \quad (1)$$

To assess fabric structure deformation during cyclic testing and evaluate its extensional deformation, an image analysis system was developed. A 20X large clip-on magnifying glass lamp was settled between a conventional digital camera (4K resolution) and the test specimen mounted on the dynamometer apparatus. In order to achieve images with identical scales, the distances between the camera, magnifying lens and test specimen were fixed for all the samples. The tests were performed at the standard illuminant D65. The obtained images were dimensioned using the Leica Application Suite 4.4 software.

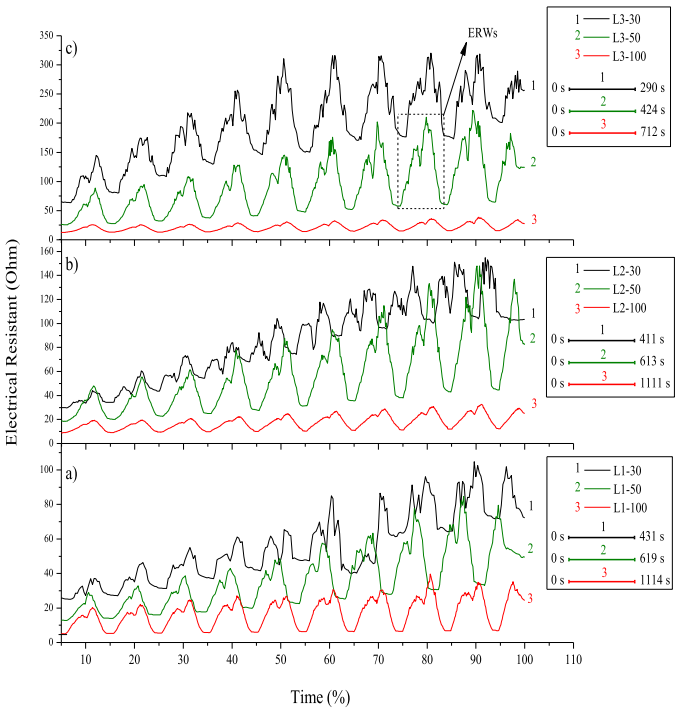

Fig. 3. Electrical resistance vs. time respect to the loop length a) L_1; b) L_2; and c) L_3. The total test durations (s) for each strain sensor are demonstrated under graph legends.

III. Results

The influence of tensile fatigue strains and loop length quantities on piezoresistive knitted-fabric sensors responses were investigated. Electrical resistance (Ω) and tensile force fatigue (N) were measured simultaneously. In the electrical resistant (ER) versus tensile fatigue time plot, the pulsed piezoresistive response was named as electrical resistant ave-form (ERW Fig.3a-c). The tensile fatigue time was expressed as the ratio (%) of time at each elongation against the total time of the tensile fatigue test. The total test time duration (s) for each sample was showed in Fig.3 insets. The fatigue tensile tests of the strain sensors performed with the same extension but at different loop lengths (i.e. L_1, L_2, L_3) showed different duration values. This behavior can be explained by the fact that knitted structure with higher longer loop length are more extensible. Therefore, considering the tested tensile fatigue elongation ranges (0-30, 0-50 and 0-100%), sample with longer loop length require additional time to be extended.

As it can be seen in Fig.3a-c, ERWs show a double-phase configuration comprising two consecutive peaks, a small and a large one. The electrical resistant amplitude of each ERW increases stepwise per each tensile fatigue cycle. The highest growth rate was observed for the sample with the lowest extension range (0-30% elongation of original length). However, it shows a disordered ERW (high noise). Samples extended to 50% of original length, exhibit acceptable waveform but the observed ERW slopes and interferences require further efforts to be improved i.e. ERWs filtration. On the other hand, by increasing the tensile strain up to 100% of the original length, the ERWs display stable waveforms. Moreover, the sensors with the highest loop length (L_3) showed the most uniform ERW configuration.

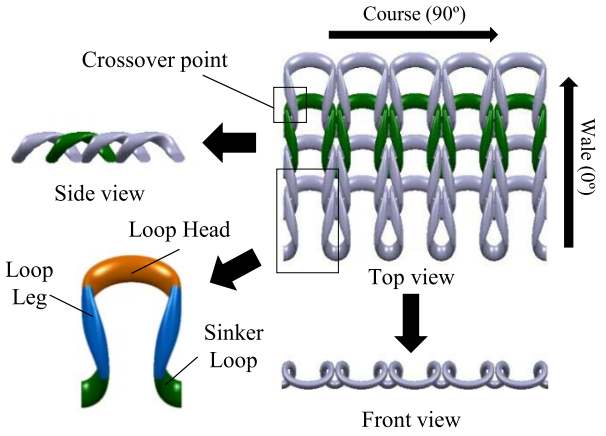

Fig. 4. structural parameters in an ordinary weft knit plain structure.

The steady ERWs in the samples with the higher tensile fatigue elongation range (0-100%) can be explained by the fact that the sample have an adequate time to release the residual stress (raised from structural deformation) accumulated in each loading-unloading cycle. Thus, the sensors with the highest extension range (100% of original length) and loop length (L_3) were selected as acceptable strain sensors due to the observed lowest noise ERWs.

IV. Discussion

Electromechanical properties of strain sensors with loading-unloading tensile cycle are linked to the structural deformation of knitted fabrics. This relationship is better verified merging the Tensile Force (N) – Time (s) with the ER (Ω) – Time (s) plots and drawing intersection lines to connect the two plots on specific points. Moreover, the observation of the elongation rate of the knit loop during tensile fatigue can also help to explain the double-phase configuration of ERWs.

Fig.4 shows the Jersey knitted fabric architecture and the loop structure, which is composed by three main sections named as head, leg and sinker. Crossover points in this structure are architecturally defined by the junction of the sinker loop and loop head (Fig.4). An increase in loop length leads to a reduction of the crossover points per sensor area. Moreover, a longer loop length in the fabric structure provides a straight configuration, which facilitate the electron path and reduce the noises in ERWs. Thus, ERW uniformity can be enhanced decreasing the number of crossover points in the knitted fabric (Fig.4).

To understand the electro-mechanical response of piezoresistive knitted sensors, the ER versus time plot of the L_3-100 sample was selected for a detailed analysis. Fig.5 displays the ER (Ω) and tensile fatigue force (N) versus time (s) plots of sensor L_3-100 for ten tensile fatigue cycles. The intersection line A represent the sensor stretching onset. From this point the ER magnitude increase reaching the first ER peak (intersection line B). Then, the ER drops reaching the minimum value at the intersection line C (Fig.5). Between intersection C and D the ER shows a minimum plateau of 10 s. Afterward, the ER return to increase while the tensile force decrease. A second ER peak is then reached at the intersection E. These peaks (intersections B and E) are

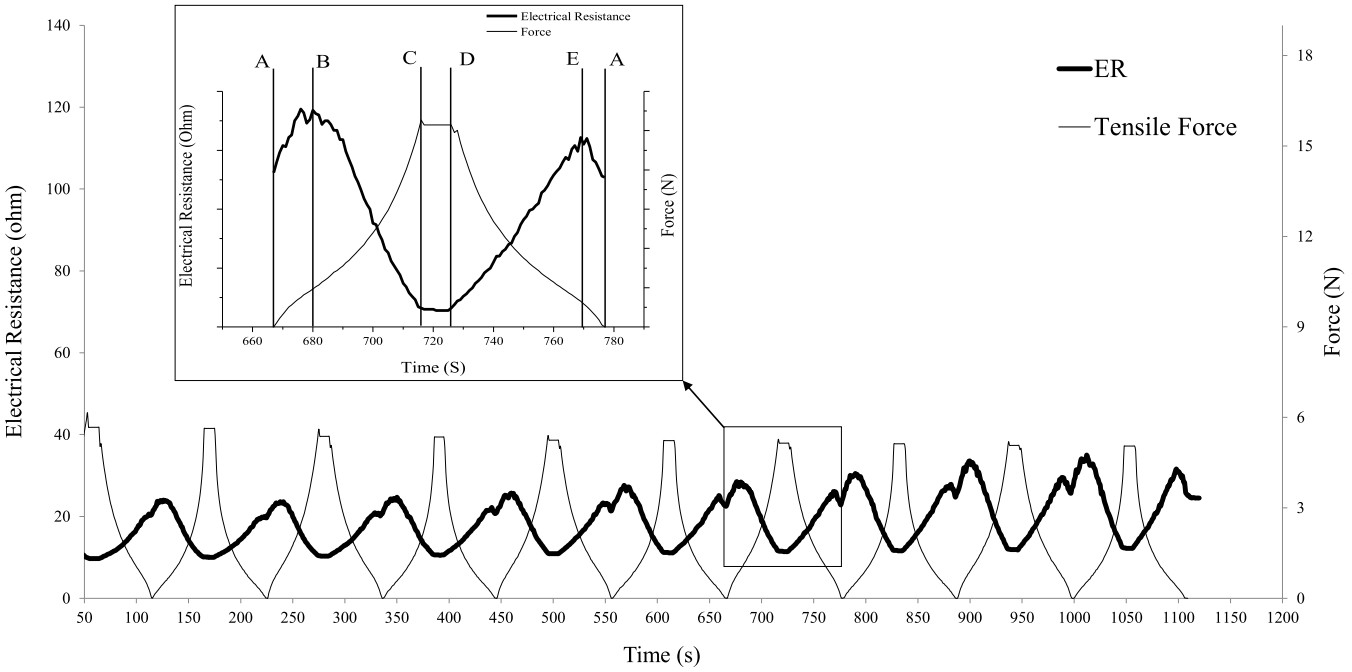

Fig. 5. Peak fitting of electrical resistance vs. time and cyclic tensile force vs. time curves for specimen L_3-100.

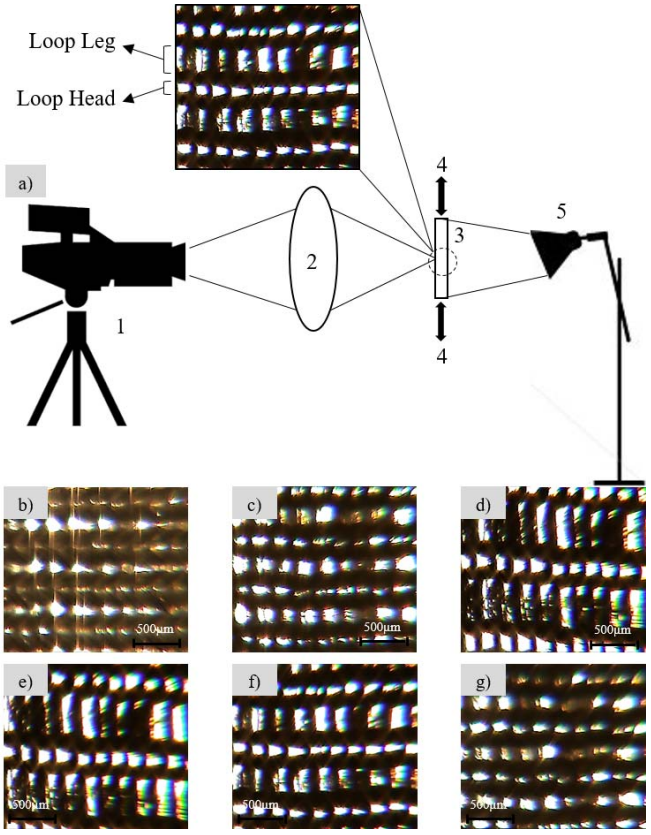

Fig. 6. a) Images capturing set and strain sensor's surface during cyclic tensile test (1- Conventional digital video camera, 2- large clip-on magnifying glass lamp (20X), 3- Test sample, 4- applied cyclic tensile force, 5- D65 (LAV/Spec. Excl., d/8, D65/10°) illumination light). b) Stretching onset (intersection point A). c) Half of stretching. d) End of stretching (intersection point B). e) relaxing onset (intersection point C). f) Half of relaxing; g); small peak of electric resistance (intersection point E).

unexpected because they correspond to the stretching onset and to the end of unloading tensile force, respectively.

The ER value decreases as the tensile force increase due to the reduction on yarn diameter in the knitted fabric structure that facilitate the electron path through the yarns. The crossover points in the knitted fabric (Fig.4) are the main responsible for transferring the fabric structural deformation to the yarns structure. Therefore, the yarn diameter reduction was identified as the main factor for reducing the ER magnitude.

The two peaks in ERWs (intersection lines B and E-Fig.5) match with the inflection points in the tensile fatigue force-time plot. Changes in sensor structure geometry during cyclic tensile test were image captured and analyzed to explain the above relationship (Fig.6). As Fig.6 shows, two distinct sections with different elongation in both loop head and leg were observed.

Fig.7 shows in detail and for just one cycle the simultaneous plot of loop leg and loop head elongations, electrical resistance and tensile fatigue force-time for L_3-100 sensor at the selected cycle 7 from Fig.5. Five defined intersection lines were drawn corresponding to the A, B, C, D and E points in Fig. 7. Moreover, the plot of loop head and leg elongation (mm) versus time (s) was divided into four specific zones representing relaxation (unloading) zone 1 and 2, and stretching (loading) zone 1 and 2. The partitioning of the plots allows explaining the unpredictable behavior of the electrical resistance at the intersection lines B and E (Fig.5). The entire procedure starts by stretching the loop leg and loop head with a different elongation rate. This stretching matches with the increase in the ER value in the ER-time plot (Fig. 7). Afterward, both loop leg and loop head are stretched showing identical elongation rate at the maximum tensile force, which also correspond to the minimum ER value (intersection C in the stretching zone 2 – Fig.7). After the plateau interval (intersections C to D) the ER magnitude increases again due to identical loop head and loop leg elongations. At the same time the

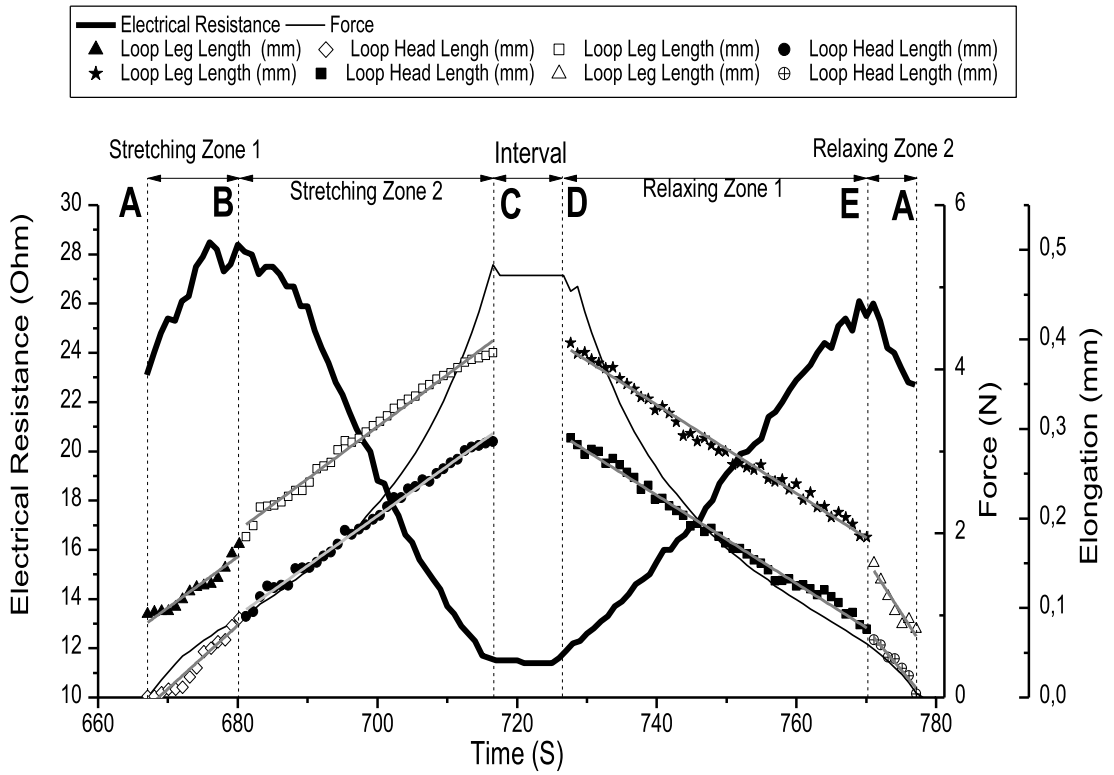

Fig. 7. Simultaneous plot of Elongation vs. time, electrical resistant vs. time and force vs. time for specimen L_3-100 at cycle seven. Inset plot of electrical resistant vs. time and force vs. time.

TABLE II
RELEVANT LINEAR REGRESSIONS EQUATIONS AND COEFFICIENT OF DETERMINATION

Zone	Loop Leg		Loop Head	
	Elongation Rate ($mm.s^{-1}$)	SD	Elongation Rate ($mm.s^{-1}$)	SD
Stretching Zone 1	57.4E-4	4.57E-4	71.7E-4	4.95E-4
Stretching Zone 2	58.7E-4	9.8E-5	56.E-42	7.23E-5
Relaxation Zone 1	-50.0E-4	8.09E-5	-49.8E-4	6.97E-5
Relaxation Zone 2	-121.9E-4	1.71E-4	-93.7E-4	8.83E-4

tensile force decreases to the inflection point (intersection line D to E - relaxing zone 1 - Fig.7). However, an unexpected drop in ER was observed (intersection line E to A - relaxing zone 2 - Fig.7). The minimum point of this drop is coincident with the minimum point of the tensile force (intersection A - relaxing zone 2 - Fig.7). After this point a new cycle begins and the tensile force as well as the ER start to increase again (intersection B -relaxing zone 2- Fig.7). In conclusion, the intersection lines B and E can be defined as the discrepancy of elongation and contraction rates of loop head and loop legs, respectively (TABLE II). Loop head extension is limited by the lateral loop sinker that increases the friction in the crossover point region. On the other hand, the loop leg can elongate more freely due to the lack of connection to the fabric structure displaying higher extensibility in stretching onset and at the end of the relaxation process.

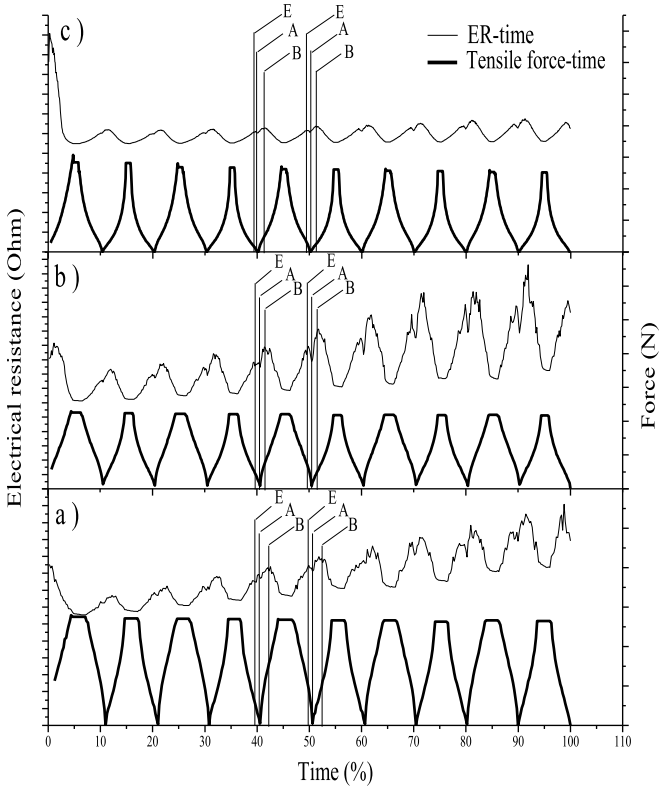

Fig. 8. Tensile fatigue (N) versus time (%) for L3 loop length a) L3-30; b) L3-50; and c) L3-100.

To understand the upward tendency of ERWs a comparison between electrical resistant and tensile fatigue-time plots for the samples with loop length L_3 was performed (Fig.8).

By increasing the extension ranges from 0-30%, 0-50% and 0-100% of the original sensor length, the ER amplitude in each ERW is expected to decline reaching a linear configuration. The tensile fatigue cycles display an alternating configuration in which the intersection lines E and B become closer and move away to intersection line A each two cycles. This distance of B and E to A is higher in the extension range of 0-100% of the original length due to the available longer time for the release of the residual stress in the fabric structure.

At low extension ranges the momentary elastic deformation corresponds to the residual stress causing a lag time. This yields to a significant change on the elongation and contraction rates of loop components in the next tensile cycle.

V. Conclusion

This work studied the influence of base fabric parameters on the electro-mechanical properties of an intrinsically conductive knitted fabrics made from stainless steel and polyester yarn under several determined extensions. The results showed a decrease in uniformity of the ERW in the case of the shortest loop length samples. Moreover, double ERW peak configuration was observed. The electrical resistance of the sample with the highest loop length showed the best applicable ERWs. A clear correspondence between electrical resistance and cyclic tensile force versus time of the sample with the highest loop length was also demonstrated. The observed discrepancies in the elongation and contraction rate of loop legs and loop heads in the knitted fabric structure during loading-unloading cycles were identified as the main reason for the generation of a double phase ERWs. The main conclusion that can be drawn from this work is that the optimum loop length and the symmetrical fabric geometry can be considered as the most important parameters to obtain a predictable ERW and ease the strain sensors optimization.

Acknowledgment

The authors would like to thank Professor Raquel Menezes for her supervision for data analysis, and Jorge Gomes Peixoto for the technical support.

References

[1] L. Ristić, *Sensor Technology and Devices*. Norwood, MA, USA: Artech House, 1994.
[2] T. Kirstein, D. Cottet, J. Grzyb, and G. Tröster, "Wearable computing systems—Electronic textiles," in *Wearable Electronics and Photonics*. Boca Raton, FL, USA: CRC Press, 2005, pp. 177–197.
[3] D. De Rossi, A. Della Santa, and A. Mazzoldi, "Dressware: Wearable hardware," *Mater. Sci. Eng. C*, vol. 7, no. 1, pp. 31–35, 1999.
[4] D. Kincal, A. Kumar, A. D. Child, and J. R. Reynolds, "Conductivity switching in polypyrrole-coated textile fabrics as gas sensors," *Synth. Met.*, vol. 92, no. 1, pp. 53–56, 1998.
[5] S. Stassi, V. Cauda, G. Canavese, and C. F. Pirri, "Flexible tactile sensing based on piezoresistive composites: A review," *Sensors*, vol. 14, no. 3, pp. 5296–5332, 2014.
[6] H. Zhang, X. Tao, T. Yu, and S. Wang, "Conductive knitted fabric as large-strain gauge under high temperature," *Sens. Actuators A, Phys.*, vol. 126, no. 1, pp. 129–140, 2006.
[7] G. E. Collins and L. J. Buckley, "Conductive polymer-coated fabrics for chemical sensing," *Synth. Met.*, vol. 78, no. 2, pp. 93–101, 1996.
[8] D. De Rossi *et al.*, "Electroactive fabrics and wearable biomonitoring devices," *AUTEX Res. J.*, vol. 3, no. 4, pp. 180–185, 2003.
[9] S. P. Armes, M. Aldissi, M. Hawley, J. G. Beery, and S. Gottesfeld, "Morphology and structure of conducting polymers," *Langmuir*, vol. 7, no. 7, pp. 1447–1452, 1991.
[10] H. H. Kuhn, W. C. Kimbrell, J. E. Fowler, and C. N. Barry, "Properties and applications of conductive textiles," *Synth. Met.*, vol. 57, no. 1, pp. 3707–3712, 1993.
[11] D. De Rossi, F. Carpi, F. Lorussi, A. Mazzoldi, E. P. Scilingo, and A. Tognetti, "5.1: Electroactive fabrics for distributed, conformable and interactive systems," in *Proc. IEEE Sensors*, vol. 2. Jun. 2002, pp. 1608–1613.
[12] A. Mazzoldi, D. De Rossi, F. Lorussi, E. Scilingo, and R. Paradiso, "Smart textiles for wearable motion capture systems," *AUTEX Res. J.*, vol. 2, no. 4, pp. 199–203, 2002.
[13] F. Carpi and D. De Rossi, "Electroactive polymer-based devices for e-textiles in biomedicine," *IEEE Trans. Inf. Technol. Biomed.*, vol. 9, no. 3, pp. 295–318, Sep. 2005.
[14] H. Zhang, X. Tao, S. Wang, and T. Yu, "Electro-mechanical properties of knitted fabric made from conductive multi-filament yarn under unidirectional extension," *Text. Res. J.*, vol. 75, no. 8, pp. 598–606, 2005.
[15] P. Xue, X. M. Tao, K. W. Y. Kwok, M. Y. Leung, and T. X. Yu, "Electro-mechanical behavior of fibers coated with an electrically conductive polymer," *Text. Res. J.*, vol. 74, no. 10, pp. 929–936, 2004.
[16] L. Zhang, G. L. Song, and K. Yang, "Study on knittability of conducting knitted fabric," *J. Tianjin Polytech. Univ.*, vol. 5, no. 5, p. 14, 2008.
[17] M. Silva, A. P. Catarino, H. Carvalho, A. Rocha, J. L. Monteiro, and G. Montagna, "Textile sensors for ECG and respiratory frequency on swimsuits," in *Proc. Intell. Textiles Mass Customisation Int. Conf.*, 2009, pp. 301–310.
[18] L. Li, M. W. Au, K. M. Wan, S. H. Wan, W. Y. Chung, and K. S. Wong, "A resistive network model for conductive knitting stitches," *Text. Res. J.*, vol. 80, no. 10, pp. 935–947, 2009.
[19] O. Atalay, W. R. Kennon, and M. D. Husain, "Textile-based weft knitted strain sensors: Effect of fabric parameters on sensor properties," *Sensors*, vol. 13, no. 8, pp. 11114–11127, 2013.
[20] B. Yang, X. Tao, J. Cai, and T. Yu, "Strain sensing behavior of textile structures made of stainless steel continuous filament yarns under uniaxial tensile loading," in *Proc. Int. Conf. Smart Mater. Nanotechnol. Eng.*, 2007, p. 642363.

Shafagh Dinparast Tohidi received the M.Sc. degree from the University of Amirkabir, Tehran, in 2009. During his M.Sc., he participated on several research projects held by Jakob Müller AG Company, Switzerland, Park of Science and Technology, Iran, and Picanol Company, Belgium. He is currently pursuing the Ph.D. degrees in textile composites with the Center of Textile Science and Technology (2C2T) and the Institute of Polymer Composite, University of Minho, Portugal. He holds a patent on a novel textile machine. He holds a Ph.D. Scholarship from the Portuguese Foundation of Science and Technology. His research interests include single polymer composites, development of 2-D and 3-D fibrous structures in reinforcing fibrous material utility, and fibrous tensile strain sensors.

Andrea Zille received the B.S. and M.S. degrees in environmental science from the University of Venice, Italy, in 2000, and the Ph.D. degree in textile chemistry engineering from the University of Minho, Portugal, in 2005. He currently leads the investigation line "Biotechnology and nanotechnology applied to materials" as a Senior Researcher with the Centre for Textile Science and Technology (2C2T), Guimarães, Portugal. He has deep knowledge in plasmatic surface treatments (DBD), applied enzymology, and nano-coating of natural and synthetic fibers. His main research activities concern the enzymatic, physical, and chemical surface modifications and functionalization of woven and non-woven materials.

André Paulo Catarino received the degree in electrical and computers engineering from the University of Porto's Faculty of Engineering in 1992, and the M.Sc. and the Ph.D. degrees in textile engineering and technology areas from the School of Engineering in 1998 and 2005, respectively. He started to work at the Textile Engineering Department, University of Minho, in 1994, where he is currently an Assistant Professor. He is also a Researcher with the Center for Textile Science and Technology (2C2T), University of Minho. His specific interests lie on knitting technology and processes, and interactive textiles, especially applied on health and sports.

Ana M. Rocha is currently an Assistant Professor of Textile Engineering and the Vice-Director of the Centre for Textile Science and Technology, University of Minho. She coordinates several research projects in the field of multifunctional and interactive textiles, namely, e-textiles and i-wear/clothing, financed by national and international programs or by companies. She supervises several M.Sc. and Ph.D. thesis. She has authored or co-authored aroundbreak 100 peer-reviewed papers and two patents. Since 2002, she has been a member of several EC expert evaluation committees in the area of smart textiles/smart materials and an expert of the European Textile Platform.